Dual roles of brushite crystals in calcium oxalate crystallization provide physicochemical mechanisms underlying renal stone formation

R Tang[1,2], GH Nancollas[1], JL Giocondi[3], JR Hoyer[4] and CA Orme[3]

[1]Department of Chemistry, The State University of New York at Buffalo, Buffalo, New York, USA; [2]Department of Chemistry, Zhejiang University, Hangzhou, Zhejiang, China; [3]Department of Chemistry and Materials Science, Lawrence Livermore National Laboratory, Livermore, California, USA and [4]University of Pennsylvania School of Medicine and The Children's Hospital of Philadelphia, Philadelphia, Pennsylvania, USA

Calcium oxalate monohydrate (COM) crystals are the major mineral component of most kidney stones, and thus have an important role in chronic human disease. However, the physicochemical mechanisms leading to calcium oxalate (CaOx) stone disease are only partially defined. As spontaneous precipitation of CaOx is rare under renal conditions, an alternative pathway for CaOx crystallization seems necessary to resolve this central issue. We performed kinetic studies using the dual constant composition method to simultaneously analyze the crystallization of COM and brushite, the form of calcium phosphate that is most readily formed in the typical slightly acidic urinary milieu. These studies were supported by parallel analysis by scanning electron and atomic force microscopy. In these studies, mineralization of a thermodynamically stable phase (COM) was induced by the presence of brushite, a more readily precipitated inorganic phase. Furthermore, once formed, the COM crystals grew at the expense of brushite crystals causing the dissolution of the brushite crystals. These studies show that brushite may play crucial roles in the formation of COM crystals. The definition of these two roles for brushite thereby provides physicochemical explanations for the initiation of COM crystallization and also for the relative paucity of calcium phosphate detected in the majority of CaOx renal stones.

Kidney International (2006) **70,** 71–78. doi:10.1038/sj.ki.5000424; published online 26 April 2006

KEYWORDS: renal stone; biomineralization; calcium oxalate; brushite; phase transformation

Correspondence: *GH Nancollas, Department of Chemistry, Natural Sciences Complex, State University of New York at Buffalo, Natural Sciences Complex, Amherst, New York 14260, USA. E-mail: ghn@buffalo.edu*

Received 16 November 2005; revised 23 February 2006; accepted 1 March 2006; published online 26 April 2006

The formation of renal stones (nephrolithiasis) is a common urinary tract disorder that often causes severe pain.[1] Renal stones are inorganic crystalline aggregates mixed with about 5% of an organic matrix. Although several combinations of crystals have been identified, the majority of stones are composed of calcium oxalate (CaOx), predominantly the monohydrate (COM); a small fraction of calcium phosphate phases is also frequently present in these COM stones.[2–4] More than half of the patients with CaOx stones have hypercalciuria.[1,5] This elevated level of calcium raises the degree of saturation for CaOx and calcium phosphate in urine.

The crystal nucleation, growth, and agglomeration of CaOx and calcium phosphate crystals in urine are strongly influenced by the levels of saturations, S. In most cases, CaOx does not precipitate as soon as the solution becomes supersaturated ($S>1$). Instead, the solution remains metastable until the supersaturation exceeds a critical value, S_c. Although $S>1$ is sufficient to drive seeded crystal growth of CaOx, *in vitro* studies have shown that homogeneous nucleation of CaOx is very improbable;[6] the level of supersaturation required to exceed the upper limit of metastability to allow the initiation of homogeneous CaOx crystallization is rare, if ever achieved in normal human urine.[7]

With the exception of the CaOx hydrates, most human urines are often undersaturated with respect to stone-forming minerals. However, changes in urinary pH and flow rate as well increased urinary calcium and/or phosphate excretion, for example, after ingestion of food may cause the calcium phosphate concentration product to become supersaturated several times a day. As supersaturation is at least transiently present, the detection of trace amounts of brushite (DCPD, $CaHPO_4 \cdot 2H_2O$) and other calcium phosphate phases in many CaOx stones[2–4] may reflect an important role for calcium phosphates in CaOx stone pathogenesis.[8,9] Brushite is not the thermodynamically most stable calcium phosphate phase. However, it is the phase that is most readily formed in slightly acidic aqueous solutions.[9,10] It is usually

considered to be a precursor for other thermodynamically more stable calcium phosphates in biomineralized tissues such as bones and teeth. As noted above, the urinary environment in patients with recurrent calcium nephrolithiasis is often supersaturated with respect to brushite.[8,9,11,12] Within the nephron, the earliest segment with high levels of supersaturation for calcium phosphates in tubular fluid is the descending thin limb of the loop of Henle.[13] This facilitates the precipitation of brushite crystals in this segment.

On the basis of these considerations, the heterogeneous nucleation and growth of CaOx on brushite crystals is a plausible initial step in the mechanism leading to the formation of CaOx stones. In the present study, we have critically examined this hypothesis using a sensitive dual constant composition (DCC) method[14,15] that simulates the complex conditions encountered in many biomineralization processes involving multiple phases. This method allows the simultaneous monitoring of the nucleation and crystal growth and/or dissolution of both brushite and COM. This analysis was augmented by our scanning electron microscopy (SEM) and atomic force microscopy (AFM) studies performed in parallel. The results unequivocally show that brushite crystals can provide sites for the heterogeneous nucleation of COM crystallites and promote their aggregation. Subsequently, the dissolution of brushite caused by a decrease of calcium ions owing to incorporation into COM provides additional calcium ions that increase the degree of CaOx supersaturation and thereby drive additional COM formation.

RESULTS

The stability of solutions for DCC studies was defined in initial studies. Metastable reaction solutions, supersaturated with respect to both brushite and COM, containing calcium, phosphate, and oxalate concentrations of 2.50, 12.00, and 8.00×10^{-2} mM, respectively, and 0.15 M NaCl, were evaluated at pH 6.0 and 37°C. The supersaturation ratios, S,[16] with respect to brushite and COM were 1.271 and 1.864, respectively. In the absence of seed crystals, these solutions remained stable with respect to brushite for at least 20 h and with respect to COM for at least 2 days without precipitation. Upon the introduction of brushite seed crystals, the addition of the two titrant solutions designed to monitor brushite growth was triggered immediately, whereas no addition of COM titrants was initially required to maintain constancy of composition. Thus, brushite was initially grown on the added seeds without any COM crystallization. Plots of titrant volume as a function of time (Figure 1) show that the brushite growth rate (calculated from the slopes of these curves) increased over time during an initial period as the total available crystal surface area was increased by growth. The addition of COM titrants reflecting nucleation and growth of this phase began only after an induction period of ~40 min (Figure 1). As soon as COM began to precipitate, the addition of brushite titrants markedly decreased, indicating that no further brushite growth was taking place while COM growth rates were accelerating (Figure 1). In control experiments in which COM seed crystals were added to this mixed system, there was only growth of COM without any growth of brushite.

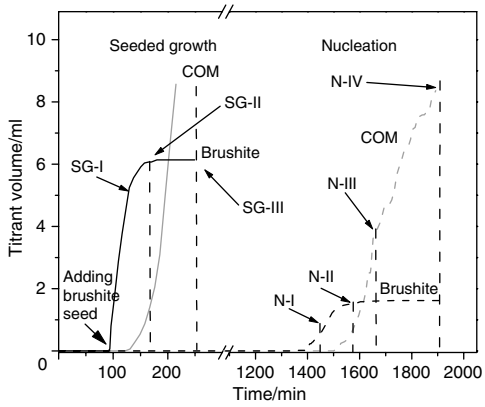

Figure 1 | DCC crystallization plots in a mixed solution of calcium phosphate ($S_{brushite} = 1.271$) and oxalate ($S_{COM} = 1.864$). In the seeded section on the left side, 20 mg of brushite seeds are added at 100 min and the growth of this phase is immediately initiated. After a further 35–45 min, COM begins to crystallize. In the nucleation studies (no seed addition), the formation of brushite is first observed after ~1400 min and the crystallization of COM begins after an additional 100–120 min. However, under identical experimental conditions but in the absence of phosphate, these COM supersaturated solutions ($S_{COM} = 1.864$) can remain metastable for more than 2 days without precipitation. Thus, the nucleation of COM is induced and promoted by brushite in these experiments. It is also noteworthy that the addition of brushite titrants is dramatically reduced to zero soon after the formation of COM crystallites in the solutions in these studies. These phenomena are reproducible (>8 parallel experiments), and provide strong evidence that COM formation is promoted in the presence of brushite.

As brushite has a lower level of supersaturation than COM in these mixed solutions, a thermodynamic rationale for the initial growth of brushite, rather than COM, was sought. Analysis of constant composition (CC) growth rate data to ascertain interfacial energy (γ_{SL})[17] indicated that brushite growth was preferred owing to its relatively low calculated interfacial energy of 4 mJ m^{-2} as compared with 13.1 mJ m^{-2} for COM.

In control non-seeded brushite nucleation experiments at $S_{brushite} = 1.271$ in the absence of oxalate, the induction period, τ, was ~1 day, less than half the COM induction period, τ, of >2 days, at $S_{COM} = 1.864$.

The non-seeded nucleation reactions in the mixed supersaturated solutions were also monitored by DCC (Figure 1). In all cases, the precipitation of brushite was observed first at ~1400 min (23.3 h), consistent with the results of the control experiment in the absence of oxalate. Addition of COM titrants began only after a further ~120 min (Figure 1). As soon as COM began to precipitate, the addition of brushite titrants markedly decreased, indicating that no further brushite growth was taking place while COM growth rates were accelerating.

During these reactions, filtered solid phases periodically withdrawn from the slurry and examined by scanning electron micrography, energy-dispersive spectroscopy and X-ray diffraction confirmed that the first formed precipitate at stage N-I of Figure 1 was pure brushite. After the second delay period, COM began to precipitate on the existing brushite surfaces. During this period, amounts of COM crystallites in the collected solids increased (Figures 2 and 3).

A notable unexpected experimental result is that at stage N-IV (Figure 1), the previously formed brushite crystallites disappeared from the precipitated solids, which were transformed into pure COM. Thus, brushite underwent dissolution, despite the fact the system remained supersaturated with respect to both brushite and COM.

Ion speciation analysis (Table 1) showed that the ionic concentrations were well maintained before COM formation. During stages N-II–N-IV, phosphate concentrations progressively increased while calcium and oxalate remained almost constant. The rise of phosphate ion concentration ($\sim$4%) is significant as DCC is designed to maintain compositions to within $\pm$2%. The genesis of the phosphate increase is best explained by release during dissolution of brushite crystallites. On the basis of titrant addition data from the non-seeded nucleation experiments, it is estimated that complete

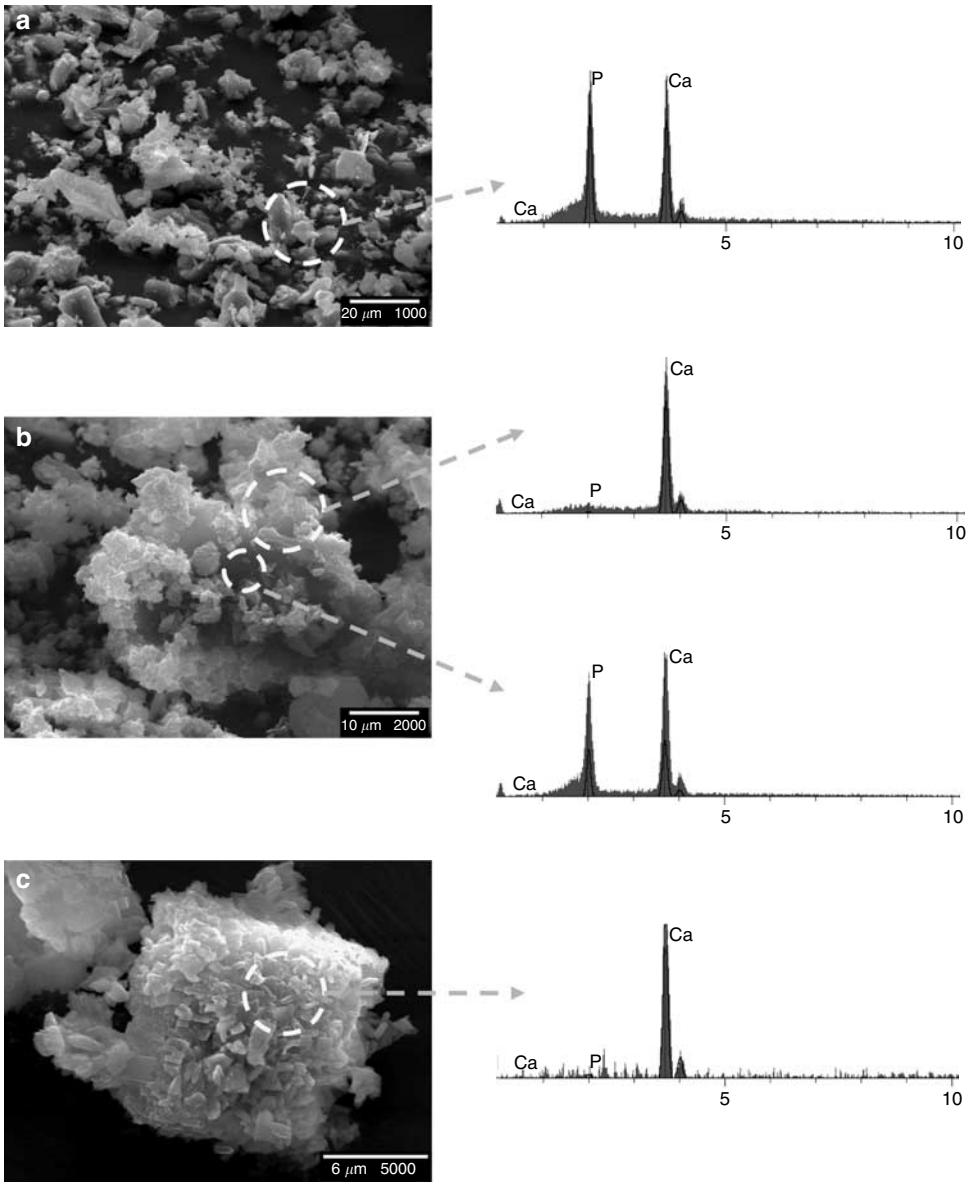

Figure 2 | SEM and energy-dispersive spectroscopy results for precipitants during the DCC nucleation experiments. (**a**–**c**) represent stages of N-I, N-II, and N-III in Figure 1, respectively. Only brushite crystallites are seen in stage N-I and COM crystallites form on the brushite surfaces at N-II. At N-III, energy-dispersive spectroscopy shows that there is no brushite on the surfaces of aggregates but that brushite can be found by X-ray diffraction after grinding, indicating that it is present in the cores. The morphologies of solids at N-IV are similar to those at N-III; however, the brushite peaks are not detected by X-ray diffraction even after grinding (see Figure 3).

dissolution of precipitated brushite crystallites would increase the phosphate concentration in the final (stage N-IV) solution by about 4.0×10^{-4} M. This is in good agreement with the chemical analysis data in Table 1. In the brushite-seeded growth studies, as 20 mg of brushite seed crystals were introduced initially, the eventual increase in the phosphate concentration is more clearly seen ($\sim$10%, Table 1) and the estimated value is also consistent with the experimental data. SEM of the solid phases in stage SG-II (Figure 4) shows the formation of COM on the dissolving brushite edges: typical smooth brushite surfaces during growth are roughened following dissolution. In stage SG-II, the total amount of brushite was consistently 27 ± 3 mg, whereas the total mass of brushite at stage SG-I, before COM nucleation, reached $\sim$40 mg. Clearly, the 13 mg loss of brushite can only be explained by its consumption into the solution. Furthermore, *in situ* AFM studies also confirm the dissolution of brushite

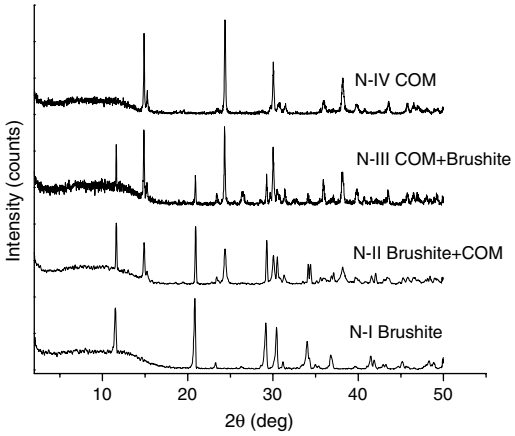

Figure 3 | X-ray diffraction of precipitated phases at different stages in the DCC nucleation studies, demonstrating that brushite dissolves after it induces COM growth.

Table 1 | Chemical analysis of filtered solids and reaction solutions during the DCC experiments

Stage	P:Ca ratio of solids	Solution/mM		
		Ca	P	Ox
N-I	1.00 ± 0.02	2.50 ± 0.02	12.00 ± 0.01	0.080 ± 0.001
N-II	0.67 ± 0.05	2.50 ± 0.03	12.10 ± 0.01	0.080 ± 0.001
N-III	0.16 ± 0.03	2.49 ± 0.03	12.30 ± 0.02	0.080 ± 0.001
N-IV	~0.0	2.48 ± 0.04	12.40 ± 0.01	0.079 ± 0.001
SG-II	0.72 ± 0.02	2.50 ± 0.03	12.20 ± 0.01	0.080 ± 0.001
SG-III	~0.0	2.49 ± 0.03	13.20 ± 0.02	0.078 ± 0.002

Abbreviations: Ca, calcium; DCC, dual constant composition; Ox, oxalate; P, phosphate.

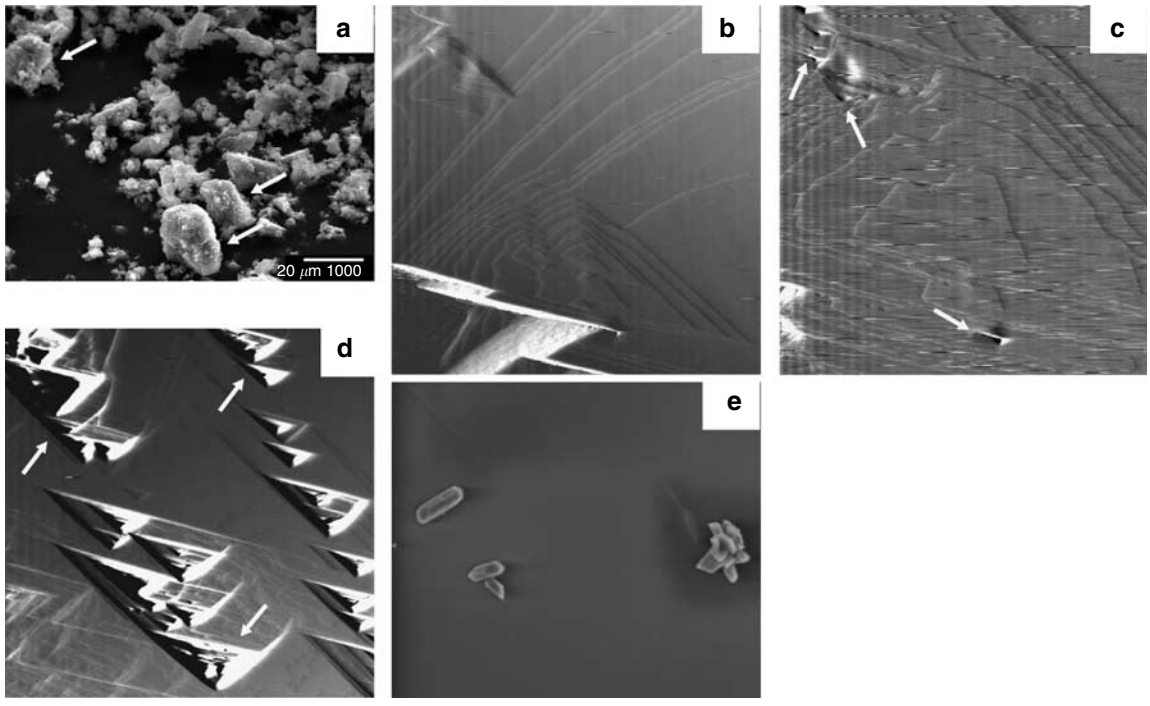

Figure 4 | SEM and AFM images show the formation of COM near the dissolving brushite surface. (**a**) SEM at stage SG-II showing numerous small COM crystallites precipitating (arrows) on the dissolving and roughened brushite surfaces. (**b**–**d**) AFM deflection images (20×20 μm). These images show the effect of oxalate on brushite (010) growth. (**b**) Brushite surface growing in solution containing 0.6 mM Ca^{2+} and 60 mM PO_4^{4-}. The triangular growth hillocks are representative of normal brushite growth. (**c** and **d**) The same area as in (**b**) in a solution containing 0.6 mM Ca^{2+}, 60 mM PO_4^{4-}, and 1.1 mM $C_2O_4^{2-}$. Brushite has become undersaturated at this oxalate concentration. (**c**) Dissolution pit (arrows) formation on the brushite surface occurs at the same time that COM particles are formed in the solution phase. The COM particles in the perfusate appear as streaks during flow. (**d**) Lower power micrograph of the development of dissolution pit (arrows) on the smooth brushite surface. (**e**) SEM showing COM particles that settled on the brushite surface after perfusion was stopped at the end of the experiment.

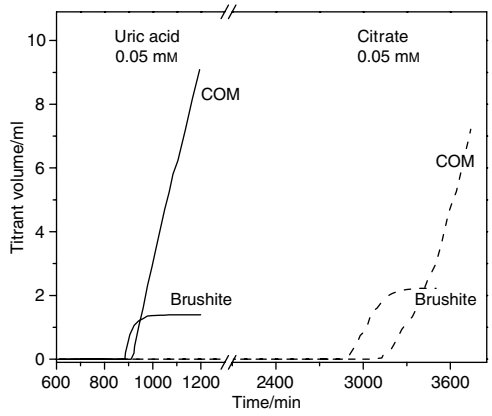

Figure 5 | DCC nucleation and crystallization plots in the presence of uric and citric acids show similar features to those in Figures 1 and 2. However, 0.05 mM uric acid promotes both brushite and COM formation. This reduces the induction time for brushite nucleation from ~13 490 to ~860 min and the time period between the nucleation of these phases to about 30 min. In contrast, 5.0×10^{-5} M citric acid inhibits both the nucleation of brushite, extending the induction period to about ~ 2900 min, almost double that in the absence of this additive and the delay period between brushite and COM formation to ~220 min.

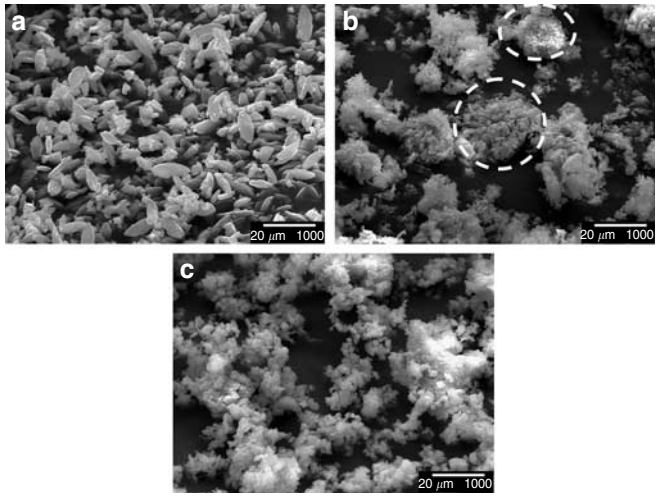

Figure 6 | (a) In the absence of brushite, the grown COM crystallites are well separated and there is no aggregation such as is seen in kidney stones. (**b**) However, COM precipitation induced by brushite in the presence of uric acid produces extensively aggregated masses similar to those observed in the renal tract. (**c**) These COM aggregates are dispersed to some extent by citrate, which also retards the crystal growth of COM.

while COM was forming (Figure 4b–e). The AFM investigation shows that (i) after immersing brushite crystallites into the reaction solution, growth of this phase was initiated as the solution was supersaturated; (ii) brushite dissolution pits were formed in the presence of high oxalate concentrations at which brushite was undersaturated (Figure 4c); (iii) dissolution of brushite continued and the pits became larger with surface roughening (Figure 4d); and (iv) COM forms in solution near the dissolving brushite surface (Figure 4b and e). This strongly suggests that brushite dissolves to provide calcium ions for COM crystallization after having induced the nucleation of this phase. It should also be noted that the induced time period of COM on brushite in the AFM studies is in agreement with that DCC bulk experimental results.

As clinical observations suggest that elevated uric acid levels and deficiencies of citrate may promote kidney stone formation,[18,19] potential roles of these urinary constituents were evaluated by *in vitro* DCC nucleation studies (Figure 5). The resulting DCC crystallization curves have similar features to those in Figure 1. However, in the presence of 0.05 mM uric acid, the crystallizations of both brushite and COM were promoted and the time period between their nucleation events was reduced to 30 min. SEMs showed that the COM crystallites nucleated on brushite crystals in a reaction solution without uric acid remained separated (Figure 6a), whereas COM crystals formed in the presence of uric acid showed extensive crystal aggregation (Figure 6b). In contrast, 0.05 mM citrate inhibited the nucleation of both brushite and COM (Figure 5). The induction period for brushite nucleation was extended to ~2900 min by 0.05 mM citrate, an interval nearly twice that in control studies without additives. Citrate also retarded the nucleation of COM on brushite surfaces; the delay period was increased to 200–240 min.

DISCUSSION

The present studies clearly demonstrate that brushite crystals serve as a very effective substrate for the heterogeneous nucleation of COM at a level of supersaturation for COM that will not lead to spontaneous precipitation. They further demonstrate that once formed under these conditions, COM crystals cause the dissolution of brushite crystallites.

In the present studies, despite a higher supersaturation for COM than brushite, the initial nucleated crystallite was brushite, rather than COM. Brushite nucleation experiments at $S_{\text{brushite}} = 1.271$ in the absence of oxalate had an induction period of ~1 day that is less than half that of more than 2 days, for COM at $S_{\text{COM}} = 1.864$. These supersaturations for brushite and COM are definitely lower than those that prevail in the urinary milieu within the more distal portions of the nephron. However, our present studies used pure solutions and supersaturations were optimized for maintaining CC so that relationships between the crystallization of COM and brushite could be most readily determined. As protein inhibitors of crystallization within urine were not present, our studies could be performed at lower levels of supersaturation than those present in urine. It should be noted that results of studies of the effects of protein inhibitors on nucleation (and growth) of COM on calcium phosphate substrates will be of obvious interest.

The existence of a critical supersaturation requirement for homogeneous nucleation has been satisfactorily explained by classical crystallization theories in terms of solid–liquid interfacial energetic controls during crystal formation in

solution. It follows that crystallization is not spontaneous until the driving force (supersaturation) is sufficiently large. Rather, a metastable condition is reached and a period of time, the induction period, τ, elapses before newly created crystals persist in the supersaturated solutions. τ is a complex quantity, but can be estimated in terms of a simplified nucleation theory,[20,21]

$$\ln \tau \propto \left[C_1 + C_2 \frac{\gamma_{SL}^3}{k^3 T^3 (\ln S)^2} \right] \quad (1)$$

In equation (1), C_1 and C_2 are independent constants, k is the Boltzmann constant, and γ_{SL} is the interfacial energy. Heterogeneous crystallization, including epitaxial overgrowth of one crystalline phase upon another, can reduce the critical supersaturations and thereby, τ. Such a mechanism is believed to play an important role in the biomineralization of extracellular structures essential for the function of the organism, such as the shells of marine organisms, bones, and teeth as well as in the pathological formation of urinary stones.[22] Thus, the shorter induction period for nucleation of brushite can be explained by classic crystallization theory on the basis of its relatively low interfacial energy (γ_{SL} in equation (1)) of $4\,mJ/m^2$ compared to $13.1\,mJ/m^2$ for COM.[17]

In solutions supersaturated with respect to each of two sparingly soluble salts, the phase having the higher solubility will be transformed to the second phase if the salts have at least one common ion. In the present *in vitro* experiment, brushite ($K_{sp} = 2.36 \times 10^{-5}\,M^2$) has a much higher solubility than COM ($K_{sp} = 2.47 \times 10^{-9}\,M^2$) so that oxalate wins the competition with phosphate for calcium as illustrated in Figure 7. When COM crystals are present in the solution, most calcium ions preferentially associate with oxalate to form COM. The results of previous CC studies showed that, at the same supersaturation, COM has a considerably higher growth rate than brushite ($\sim 4 \times 10^{-4}\,mol\,m^{-2}\,min^{-1}$ as compared with $\sim 5 \times 10^{-5}\,mol\,m^{-2}\,min^{-1}$).[15,23] It follows that COM may readily form on dissolving brushite surfaces (Figure 4). As COM is much less soluble in the aqueous solution, this explains why no brushite growth occurs if the seed crystals are COM in the above experiment. Moreover, after COM is nucleated, the addition of brushite titrants in the DCC experiments is greatly retarded and will eventually stop as was observed experimentally.

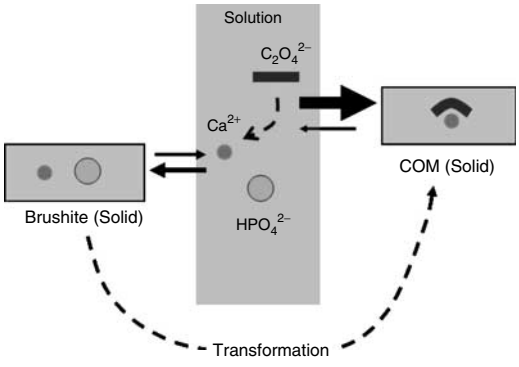

Figure 7 | Scheme showing the dynamic process based on preferential association of calcium ions with oxalate to form COM and the release of phosphate from brushite.

Brushite surfaces are good substrata for COM formation owing to high local calcium concentrations (Figure 2b). It is then possible for these COM crystallites to aggregate to form concretions that could ultimately evolve into kidney stones. However, in the control experiments, using COM as seed crystals or during nucleation in the mixed supersaturated solutions, the COM crystallites remained separated (Figure 6a). *In vivo* this would suggest, as in Figure 6b, that the brushite is located at the core of COM crystals, a position frequently encountered in kidney stones.[2,3] Over time, all of the brushite may be transformed into COM (stage N-IV of Figure 1).

In many CaOx kidney stones, there is a relatively abrupt layer to layer change in composition involving mineral phases as well as the organic components, which may include uric acid.[18,24] The precipitation sequences observed in the presences of uric and citric acids may clarify earlier concepts of kidney stone formation and prevention. It is noteworthy that the '*in vitro*' concretions formed in the presence of uric acid resemble those of stones formed in the renal tract. By contrast, citrate retarded the precipitation of brushite and COM and also reduced the aggregation of the resulting COM (Figure 6c). These observations are consistent with recent observations that citrate increases the upper limit of metastability for brushite, that is, the point at which spontaneous precipitation occurs, both directly and by increasing pH.[25] Citrate also directly inhibits the growth of COM crystals.[26]

Consideration of the present studies in relation to studies of Randall's plaques may further illuminate the sequence of events leading to CaOx stone formation. These plaques are sites of interstitial calcium phosphate crystal deposition at or near the papilla tip. The initial site of formation of Randall's plaques was recently reported to be in the basement membranes of thin loops of Henle.[27] This finding is of particular note, as this is the earliest site within the nephron of very high calcium phosphate supersaturation,[13] and under slightly acidic conditions would favor brushite formation. Furthermore, collagen, such as that in basement membranes, has been shown to precipitate brushite from urine.[28] As brushite is less thermodynamically stable than hydroxyapatite, conversion to hydroxyapatite over time is a likely basis for the detection of hydroxyapatite, rather than brushite in Randall's plaques.[27] The hypothesis that Randall's plaques are important in the initiation of CaOx stone disease is consistent with the observation that the number of CaOx stones formed correlated with the amount of papillary surface covered by plaque.[29] This hypothesis is also consistent with our previous observations showing that COM is nucleated by apatite.[16] These calcium phosphate crystals attached within the kidney provide not only a site for the

nucleation of CaOx crystals but also an attachment that allows them to increase to a size that will be retained within the urinary system.

Conclusions

The present studies rationalize a central role for brushite in the formation of CaOx stones and suggest mechanisms whereby citrate and uric acid may influence this pathogenetic sequence. The DCC data obtained under well-controlled experimental conditions provides the basis for improved understanding of the role of calcium phosphate phases in the physical chemical mechanisms responsible for kidney stone formation. Use of the DCC method allows us to unequivocally show that mineralization of a thermodynamically stable phase (COM) can be induced by another more readily precipitated inorganic phase (brushite). Furthermore, once formed, the COM crystals grow at the expense of brushite crystals causing their dissolution and thereby providing a physicochemical basis for the relative ratios of CaOx to calcium phosphate detected in the majority of renal stones.

MATERIALS AND METHODS

DCC

The (CC) method can mimic *in vivo* biologically stabilized milieux for crystallization.[14] Titrant solutions are added to maintain constant reaction solution concentrations during the experiments and the growth kinetics can be calculated from the titrant addition rates. A potentiometer is used to control titrant addition from stepper-motor-driven burets. Reaction initiation triggered, potentiometrically, the addition of titrant solutions, having concentrations calculated based upon the speciation computations using mass balance and electroneutrality expressions together with the extended Debye–Hückel equation.

In nature, simultaneous processes occurring in crystal suspension are not rare. The DCC method (two CC devices incorporating two different ion selective sensors) is used to simultaneously control both crystallization processes at constant driving force.[16] In this case, representing COM and brushite by BA and BC, respectively, they share a common B ion (calcium). For the simultaneous growth of BA and BC crystals, B ion (calcium ion-specific electrode (Orion 93-20)) and C ion (pH electrode (Orion 91-01), as $HPO_4^{2-} + H^+ \rightarrow H_2PO_4^-$) selective electrodes are used to control BA and BC titrants, respectively. The rate of reactions of BA and BC can be calculated from the corresponding recorded titrant curves. Under certain conditions, as two phases (BA and BC) grow, the change in the concentration $[X]$ [where $X = $ B, A, or C] from a set point value $[X]s$ will register a potential difference, ΔE, on the potentiometer sensed by the electrodes. When the magnitude of ΔE exceeds the electrode response thresholds, ΔE_0, addition of titrants will be triggered in order to compensate for the changes in concentration. The relative concentration variation, ε, can be written as

$$\varepsilon = \frac{[X] - [X]_s}{[X]_s} = \exp\left(\frac{zF\,\Delta E_0}{RT}\right) - 1 \qquad (2)$$

where z is the charge of the ion sensed by the electrode, and R, T, and F are the gas constant, absolute temperature, and Faraday constant, respectively. Thus, the value of ε depends on the valence of the controlled ion and the potentiometric response threshold. The rates of DCC reactions may be calculated using the method described below. The time elapsed, dt_1, before BA titrant addition is given by

$$dt_1 = \frac{\varepsilon_B [B]_s V}{R_{BA} + R_{BC}} \qquad (3)$$

in which, V is the volume of the reaction solution, and R_{BA} and R_{BC} are the overall reaction rates for phases BA and BC, respectively. It can be seen that dt_1 is the time required for species $[B]$ to reach the set point value $[B]_s$ owing to crystal growth. The volume of added BA titrant, dV_1 (dV is the volume of a single titrant buret), needed to restore $[B]$ to its original value, $[B]_s$, is given by

$$dV_1 = \frac{\varepsilon_B [B]_s V}{C_{eBA}} \qquad (4)$$

where C_{eBA} is the effective BA titrant concentration. After a time interval dt_2, the change in $[C]$ is sufficient to trigger the addition of BC titrant according to

$$dt_2 = \frac{\varepsilon_C [C]_s V}{R_{BC}} \qquad (5)$$

and volume of BC titrant added, dV_2, is given by

$$dV_2 = \frac{\varepsilon_C [C]_s V}{C_{eBC}} \qquad (6)$$

where C_{eBC} is the effective BC titrant concentration. As the change in $[C]$ is produced by the growth of only the BC phase, BC titrant addition will be controlled by the C sensor as if only this phase undergoes reaction in the system. From equations (5) and (6), the rate for the BC crystal can then be determined using

$$R_{BC} = C_{eBC} \frac{dV_2}{dt_2} \qquad (7)$$

In the time interval dt_2, there would be $\varepsilon_C\,dt_2/\varepsilon_B\,dt_1$ pulses of BA titrant addition, depending upon the electrode sensitivity. However, partial consumption of $[B]$ caused by the BC phase has already been compensated for by the addition of BAC titrants in dt_2, which will reduce the amount of BA titrant addition. Therefore, the total volume, dV_{BA}, of BA titrant required in the time period dt_2 will be given by

$$dV_{BA} = dV_1 \frac{\varepsilon_C\,dt_2}{\varepsilon_B\,dt_1} dV_2 \frac{C_{eBC}}{C_{eBA}} \qquad (8)$$

Rearranging equation (8) and introducing equations (3) and (4), we obtain

$$\begin{aligned} \varepsilon_B C_{eBA} \frac{dV_{BA}}{dt_2} &= \varepsilon_C C_{eBA} \frac{dV_1}{dt_1} - \varepsilon_B C_{eBC} \frac{dV_2}{dt_2} \\ &= \varepsilon_C R_{BA} + \varepsilon_C R_{BC} - \varepsilon_B R_{BC} \end{aligned} \qquad (9)$$

In equation (9), dV_{BA}/dt_2 is the overall slope of the BA titrant volume–time plot. Thus, the reaction rates of BA and BC can be calculated from the corresponding recorded curves if $\varepsilon_B = \varepsilon_C$, which is precisely maintained by computer during the simultaneous crystal growth and the individual DCC curves for BA and BC phases can be calculated.

I. COM (BA) phase/controlled by calcium electrode:

Titrant buret no. 1

$$\begin{cases} T_{CaCl_2} = 2W_{CaCl_2} + C_{eff,COM} \\ T_{NaCl} = 2W_{NaCl} - 2C_{eff,COM} \end{cases}$$

Titrant buret no. 2

$$\begin{cases} T_{K_2Ox} = 2W_{K_2Ox} + C_{eff,COM} \\ T_{KOH} = 2W_{KOH} \text{ and } T_{KH_2PO_4} = 2W_{KH_2PO_4} \end{cases}$$

II. Brushite (BC) phase/controlled by glass electrode:

Titrant buret no. 1

$$\begin{cases} T_{CaCl_2} = 2W_{CaCl_2} + C_{eff,brushite} \\ T_{NaCl} = 2W_{NaCl} - 2C_{eff,brushite} \end{cases}$$

Titrant buret no. 2

$$\begin{cases} T_{KH_2PO_4} = 2W_{KH_2PO_4} + C_{eff,brushite} \\ T_{KOH} = 2W_{KOH} + 2C_{eff,brushite} \text{ and } T_{KH_2Ox} = 2W_{K_2Ox} \end{cases}$$

where W and T are the total concentrations in the reaction solutions and titrants, respectively, $C_{eff,COM}$ and $C_{eff,brushite}$ are the effective titrant concentrations with respect to COM and brushite, respectively.

In situ AFM

The images were collected in contact mode using Mulitmode AFM with Nano III controller (Vecco). All images were acquired in height and deflection modes using the lowest tip force possible to reduce the tip–surface interaction. The brushite seed crystal was anchored inside the fluid cell and supersaturated solutions (identical to the DCC reaction solutions) were passed through it while the images were taken.

Scanning electron microscopy

Solid samples, under vacuum, were sputter-coated with a thin carbon deposit to provide conductivity, and then examined using a field-emission SEM (Hitachi S-4000), typically at 20 or 30 KeV.

ACKNOWLEDGMENTS

These studies were supported by research grants from the National Institutes of Health (DE03223, DK33501, and DK61673). Part of this work (CAO, JLG) was performed under the auspices of the US Department of Energy by the University of California, Lawrence Livermore National Laboratory under Contract No. W-7405-Eng-48.

REFERENCES

1. Coe FL, Parks JH, Asplin JR. The pathogenesis and treatment of kidney stones. *N Engl J Med* 1992; **327**: 1141–1152.
2. Herring LC. Observations on analysis of ten thousand urinary calculus. *J Urol* 1962; **88**: 545–555.
3. Mandel G, Mandel N. Analysis of stones. In: Coe FL, Favus MJ, Pak CYC, Parks JH, Preminger GM (eds). *Kidney Stones: Medical and Surgical Management*. Lippincott-Raven: Philadelphia, PA, USA, 1996, pp 323–335.
4. Prien EL, Prien Jr EL. Composition and structure of urinary stone. *Am J Med* 1968; **45**: 654–672.
5. Breslau NA. Pathogenesis and management of mypercalciuric nephrolithiasis. *Miner Electrolyte Metab* 1994; **20**: 328–339.
6. Finlayson B. Physicochemical aspects of urolithiasis. *Kidney Int* 1978; **13**: 344–360.
7. Asplin JR, Parks JH, Coe FL. Dependence of upper limit of metastability on supersaturation in nephrolithiasis. *Kidney Int* 1997; **52**: 1602–1608.
8. Pak CYC. Physicochemical basis for formation of renal stones of calcium phosphate origin. *J Clin Invest* 1969; **48**: 1914–1922.
9. Pak CYC, Eanes ED, Ruskin B. Spontaneous precipitation of brushite in urine: evidence that brushite is the nidus of renal stones originating as calcium phosphate. *Proc Natl Acad Sci USA* 1971; **68**: 1456–1460.
10. LeGeros RZ. *Calcium Phosphates in Oral Biology and Medicine*. Karger: Basel (Switzerland), 1991, pp 54–55.
11. Pylypchuk G, Ehrig U, Wilson DR. Idiopathic calcium nephrolithiasis. 1. Differences in urine crystalloids, urine saturation with brushite and urine inhibitors of calcification between persons with and persons without recurrent kidney stone formation. *Can Med Assoc J* 1979; **120**: 658–662.
12. Pak CYC, Hayashi Y, Finlayson B *et al.* Estimation of the state of saturation of brushite and calcium oxalate in urine: a comparison of three methods. *J Lab Clin Med* 1977; **89**: 891–901.
13. Asplin JR, Mandel NS, Coe FL. Evidence of calcium phosphate supersaturation in the loop of Henle. *Am J Physiol* 1996; **270**: F604–F613.
14. Tomson MB, Nancollas GH. Mineralization kinetics: A constant composition approach. *Science* 1978; **200**: 1059–1060.
15. Ebrahimpour A, Zhang J, Nancollas GH. Dual constant composition method and its application to studies of phase transformation and crystallization of mixed phases. *J Crystal Growth* 1991; **113**: 83–91.
16. Ebrahimpour A, Perez L, Nancollas GH. Induced crystal growth of calcium oxalate monohydrate at hydroxyapatie surfaces. The influence of human serum albumin, citrate and magnesium. *Langmuir* 1991; **7**: 577–583.
17. Wu W, Nancollas GH. Determination of interfacial tension from crystallization and dissolution data: A comparison with other methods. *Adv Colloid Interface Sci* 1999; **79**: 229–279.
18. Gambaro G, Favaro S, Borsatti A *et al.* Juvenile renal stone disease: A study of urinary promoting and inhibiting factors. *J Urol* 1983; **130**: 1133–1135.
19. Pak CYC. Citrate and renal calculi; an update. *Miner Electrolyte Metab* 1994; **20**: 371–377.
20. Walton AG. The Nucleation of sparingly soluble salts from solution. *Anal Chim Acta* 1963; **29**: 434–441.
21. Mullin JW, Ang HM. Nucleation characteristics of aqueous nickel ammonium-sulfate solutions. *Faraday Discus* 1976; **61**: 141–148.
22. De Yoreo JJ, Vekilov P. Principles of crystal nucleation and growth. In: Dove PM, De Yoreo JJ, Weiner S (eds). *Biomineralization*. Mineralogical Society of America: Washington, DC, 2003, pp 57–93.
23. Singh RP, Gaur SS, Sheehan ME *et al.* Crystal growth of calcium oxalate monohydrate. *J Crystal Growth* 1988; **87**: 318–324.
24. Asplin JR, Lingeman J, Kahnoski R *et al.* Metabolic urinary correlates of calcium oxalate dihydrate in renal stones. *J Urol* 1998; **159**: 664–668.
25. Greischar A, Nakagawa Y, Coe FL. Influence of urine pH and citrate concentration on the upper limit of metastability for calcium phosphate. *J Urol* 2003; **169**: 867–870.
26. Qiu SR, Wierzbicki A, Orme CA *et al.* Molecular modulation of calcium oxalate crystallization by osteopontin and citrate. *Proc Natl Acad Sci USA* 2004; **101**: 1811–1815.
27. Evan AP, Lingeman JE, Coe FL *et al.* Randall's plaque of patients with nephrolithiasis begins in basement membranes of thin loops of Henle. *J Clin Invest* 2003; **111**: 607–616.
28. Pak CY, Ruskin B. Calcification of collagen by urine *in vitro*: dependence on the degree of saturation of urine with respect to brushite. *J Clin Invest* 1970; **49**: 2353–2561.
29. Kim SC, Coe FL, Tinmouth WW *et al.* Stone formation is proportional to papillary surface coverage by Randall's plaque. *J Urol* 2005; **173**: 117–119.